J|A|C|S
ARTICLES

Published on Web 04/29/2009

# On the Origin of the Cobalt Particle Size Effects in Fischer−Tropsch Catalysis

J. P. den Breejen,[†] P. B. Radstake,[†,‡] G. L. Bezemer,[†,§] J. H. Bitter,[†] V. Frøseth,[‡,||] A. Holmen,[‡] and K. P. de Jong*[,†]

*Inorganic Chemistry and Catalysis, Debye Institute for NanoMaterials Science, Utrecht University, NL-3508 TB Utrecht, P.O. Box 80003, The Netherlands, and Department of Chemical Engineering, Norwegian University of Science and Technology (NTNU), N-7491 Trondheim, Norway*

Received February 9, 2009; E-mail: K.P.deJong@uu.nl

***Abstract:*** The effects of metal particle size in catalysis are of prime scientific and industrial importance and call for a better understanding. In this paper the origin of the cobalt particle size effects in Fischer−Tropsch (FT) catalysis was studied. Steady-State Isotopic Transient Kinetic Analysis (SSITKA) was applied to provide surface residence times and coverages of reaction intermediates as a function of Co particle size (2.6−16 nm). For carbon nanofiber supported cobalt catalysts at 210 °C and $H_2/CO = 10$ v/v, it appeared that the surface residence times of reversibly bonded $CH_x$ and $OH_x$ intermediates increased, whereas that of CO decreased for small (<6 nm) Co particles. A higher coverage of irreversibly bonded CO was found for small Co particles that was ascribed to a larger fraction of low-coordinated surface sites. The coverages and residence times obtained from SSITKA were used to describe the surface-specific activity (TOF) quantitatively and the $CH_4$ selectivity qualitatively as a function of Co particle size for the FT reaction (220 °C, $H_2/CO = 2$). The lower TOF of Co particles <6 nm is caused by both blocking of edge/corner sites and a lower intrinsic activity at the small terraces. The higher methane selectivity of small Co particles is mainly brought about by their higher hydrogen coverages.

## Introduction

Particle size effects in nanocatalysis are of growing interest. For both supported and unsupported particles (e.g., colloids) various examples are known where the catalytic performance was proven to be dependent on particle size and shape.[1−4] A growing number of studies are conducted to understand the nature of these effects, which is increasingly facilitated by well-defined preparation routes, support materials, surface science studies, and *ab initio* calculations.

A prime example of particle size effects is displayed in the Fischer−Tropsch (FT) reaction.[5−16] In this reaction CO and $H_2$ (syngas) are converted into hydrocarbons, which can be used for the production of clean automotive fuels. Since syngas can be obtained from various sources, including coal, natural gas, and biomass, an alternative to crude oil is provided. The FT reaction is therefore of eminent interest to both industry and academia.[17−23]

Supported cobalt catalysts are well-known for their activity and selectivity in the Fischer−Tropsch reaction. For these catalysts, the effects of particle size have been studied by various authors with original contributions from Bartholomew[8] and Yermakov.[9] Studies of Iglesia and co-workers showed that the surface-specific activity (Turnover Frequency, TOF) is not a function of the cobalt particle size in the size range 9 to 200 nm,[17] which was confirmed by others.[14,24] For smaller (<10 nm) Co particles, however, a decrease in FT performance has been

[†] Utrecht University.
[‡] Norwegian University of Science and Technology.
[§] Present address: Shell Global Solutions, P.O. Box 38000, 1030 BN, Amsterdam, The Netherlands.
[||] Present address: StatoilHydro Mongstad, N-5954 Mongstad, Norway.

(1) Che, M.; Bennett, C. O. *Adv. Catal.* **1989**, *36*, 55–172.
(2) Henry, C. R. *Surf. Sci. Rep.* **1998**, *31*, 231–325.
(3) Somorjai, G.; Tao, F.; Park, J. *Top. Catal.* **2008**, *47*, 1–14.
(4) Van Santen, R. A. *Acc. Chem. Res.* **2009**, *42*, 57–66.
(5) King, D. L. *J. Catal.* **1978**, *51*, 386–397.
(6) Jung, H. J.; Walker, P. L.; Vannice, A. *J. Catal.* **1982**, *75*, 416–422.
(7) Boudart, M.; McDonald, M. A. *J. Phys. Chem.* **1984**, *88*, 2185–2195.
(8) Reuel, R. C.; Bartholomew, C. H. *J. Catal.* **1984**, *85*, 78–88.
(9) Lisitsyn, A. S.; Golovin, A. V.; Kuznetsov, V. L.; Yermakov, Y. I. *J. Catal.* **1985**, *95*, 527–38.
(10) Jones, V. K.; Neubauer, L. R.; Bartholomew, C. H. *J. Phys. Chem.* **1986**, *90*, 4832–4839.
(11) Barbier, A.; Tuel, A.; Arcon, I.; Kodre, A.; Martin, G. A. *J. Catal.* **2001**, *200*, 106–116.
(12) Bezemer, G. L.; Van Laak, A.; Van Dillen, A. J.; De Jong, K. P. *In Stud. Surf. Sci. Catal.* **2004**, *147*, 259–264.
(13) Barkhuizen, D.; Mabaso, I.; Viljoen, E.; Welker, C.; Claeys, M.; Van Steen, E.; Fletcher, J. C. Q. *Pure Appl. Chem.* **2006**, *78*, 1759–1769.
(14) Bezemer, G. L.; Bitter, J. H.; Kuipers, H. P. C. E.; Oosterbeek, H.; Holewijn, J. E.; Xu, X.; Kapteijn, F.; Van Dillen, A. J.; De Jong, K. P. *J. Am. Chem. Soc.* **2006**, *128*, 3956–3964.
(15) Martinez, A.; Prieto, G. *J. Catal.* **2007**, *245*, 470–476.
(16) Xiao, C.-X.; Cai, Z.-P.; Wang, T.; Kou, Y.; Yan, N. *Angew. Chem.* **2008**, *120*, 758–761.
(17) Iglesia, E. *Appl. Catal., A* **1997**, *161*, 59–78.
(18) Schulz, H. *Appl. Catal., A* **1999**, *186*, 3–12.
(19) Liu, Z. P.; Hu, P. *J. Am. Chem. Soc.* **2002**, *124*, 11568–11569.
(20) Dry, M. E. *Catal. Today* **2002**, *71*, 227–241.
(21) Khodakov, A. Y.; Chu, W.; Fongarland, P. *Chem. Rev.* **2007**, *107*, 1692–1744.
(22) van Steen, E.; Claeys, M. *Chem. Eng. Technol.* **2008**, *31*, 655–666.
(23) Khodakov, A. Y. *Catal. Today* **2008**, DOI:10.1016/j.cattod.2008.10.036.

  

reported. Barbier et al. found a decrease in TOF for Co particles smaller than 6 nm for a Co on a silica catalyst.[11] Using cobalt on carbon nanofiber (CNF) catalysts, tested at both 1 and 35 bar, Bezemer et al. showed that cobalt particles smaller than 6 nm (1 bar) or 8 nm (35 bar) displayed a significantly lower TOF than catalysts with larger particles.[12,14] Together with a decrease in TOF for smaller particles, an increase in methane selectivity was observed by these authors.[14] Work by Martinez and Prieto displayed a similar particle size effect, with the use of catalysts prepared via a colloidal route.[15] A more recent study by Borg et al. emphasized the effect of the cobalt particle size on selectivity.[25]

The origin of a lower activity and selectivity of small Co particles is a longstanding scientific question. To reveal details of this origin we made use of steady-state isotopic transient kinetic analysis (SSITKA).[26−28] This technique has been applied to a variety of heterogeneous catalytic reactions, as for example summarized in a review from Shannon and Goodwin,[29] to answer questions related to surface chemistry. SSITKA is used to study steady-state surface reactions *in situ* and allows determination of the coverage and surface residence time of species involved in a specific reaction. Its usefulness has been proven especially for the Fischer−Tropsch reaction.[30−35] During the steady-state FT reaction, isotopic switches (e.g., from $^{12}CO$ to $^{13}CO$) are performed, and subsequently the isotopically labeled products and reactants are monitored as a function of time. Thus it becomes possible to deconvolute contributions to the total TOF, which is, assuming a first-order reaction, the product of an intrinsic rate constant ($k$) and coverage ($\theta$).

In the present work, the surface coverages and residence times of carbon, oxygen, and hydrogen containing intermediates and reactants are extensively studied for Co/CNF catalysts with cobalt particle sizes ranging from 2.6 to 16 nm. Carbon nanofibers are used as support to allow study of the intrinsic properties of the cobalt particles. This is possible since graphitic carbon fibers are chemically inert, in contrast to oxidic supports where poorly reducible mixed oxides may interfere during catalyst synthesis or FT catalysis. To facilitate the study, methanation conditions ($H_2/CO = 10$) are applied to minimize the number of labeled products. Yet, it is proven that the conclusions drawn are relevant for Fischer−Tropsch conditions.

## Experimental Section

**Catalyst Preparation and Characterization.** Fishbone-type carbon nanofibers (CNF) with a typical diameter of 30 nm were obtained from $CO/H_2$ at 550 °C using a 5 wt% $Ni/SiO_2$ growth catalyst (sieve fraction 90−150 $\mu$m).[36] The as-synthesized fibers were purified with successive reflux steps in 1 M KOH for 1 h and in concentrated $HNO_3$ for 2 h. In the last reflux step, also oxygen-containing surface groups were introduced, which has been proven to be indispensable to obtain high metal dispersions.[37]

Cobalt catalysts were prepared via incipient wetness impregnation. Cobalt particle sizes in a range of 2.6 to 16 nm were obtained by varying the cobalt loading (1−22 wt%), cobalt precursor (cobalt nitrate or cobalt acetate), or solvent (water or ethanol).[14] The impregnated catalyst precursors were dried overnight at 120 °C. Next, the catalysts were reduced at 350 °C under a flow of 30% $H_2/N_2$ and subsequently passivated using a diluted (0.1 vol%) oxygen flow.

Transmission Electron Microscopy (TEM), $H_2$-chemisorption, and quantitative X-ray Photoelectron Spectroscopy (XPS) were used previously to determine the cobalt particle sizes.[14] These analysis techniques delivered consistent particle sizes. X-ray absorption studies indicated that the Co particles were, within the experimental error, metallic during FT reaction at 1 bar of pressure of $H_2/CO$. Deactivation due to sintering has been excluded in previous work.[14]

**Transient Isotope Experiments.** The SSITKA apparatus used in this study has been described before.[38] To perform an experiment, typically 100 mg of catalyst (90−150 $\mu$m) were diluted with 200 mg of SiC (75−150 $\mu$m) and loaded in a plug flow microreactor. An *in situ* reduction was performed under a flow of 10 mL·min$^{-1}$ $H_2$ at 350 °C (heating rate of 5 °C·min$^{-1}$) and 1 bar for 2 h. Subsequently, the reactor was cooled to 170 °C under the $H_2$ flow. At this temperature, the flow was switched to syngas ($^{12}CO/H_2/Ar = 1.5/15/33.5$ mL·min$^{-1}$) and the pressure was increased to 1.85 bar. The temperature was raised to 210 °C, and the reaction was performed for at least 15 h prior to A SSITKA experiment.

The amount and fractions of $C_1-C_7$ hydrocarbons, CO, $H_2$, and Ar in the effluent were determined using an HP5890 gas chromatograph (GC) equipped with FID and TCD. The surface-specific activity (TOF, $10^{-3}$ $mol_{CO}\cdot mol_{Co,surf}^{-1}\cdot s^{-1}$) was calculated based on the amount of CO consumed (TCD) and hydrocarbons formed (FID). The selectivity was also based on the latter results. The presence and amount of $H_2O$ and $CO_2$ were checked with a mass spectrometer.

After reaching steady-state conditions (15 h), a switch from $^{12}CO/H_2/Ar$ to $^{13}CO/H_2/Kr$ was performed. A backswitch was made at isotopic steady state conditions. The transients in $^{13}CO$ and $^{12}CO$, the main products $^{12}CH_4$ and $^{13}CH_4$, and the inert tracers were monitored with a Balzers QMG 422 quadrupole mass spectrometer (MS). From the MS signals during the backswitch, the surface residence times ($\tau$) were calculated via the area under the normalized transient curves $F_i(t)$, and corrected for the gas phase hold-up with the use of the Ar or the Kr inert tracer.

$$\tau_i = \int_0^\infty F_i(t)\,\mathrm{d}t \tag{1}$$

The $CH_x$ residence time was corrected for the chromatographic effect of CO using eq 2.[39]

$$\tau_{CH_x(corrected)} = \tau_{CH_4(measured)} - 0.5\tau_{CO} \tag{2}$$

It is important to note that $CH_x$ represents the surface intermediates leading to methane and it is obtained from $CH_4$ transients using eq 2. The number of the reversibly adsorbed CO and $CH_x$ species could be estimated from the residence time ($\tau$) and exit flow (Q) of those species.

$$N_i = \tau_i Q_{i,exit} \tag{3}$$

The coverage of the different species was calculated by dividing the number of the relevant adsorbed species by the number of Co surface atoms. For the determination of the oxygen ($OH_x$) intermediates, an isotopic switch from $C^{16}O/H_2/Ar$ to $C^{18}O/H_2/Kr$ was performed, followed by a backswitch. The $H_2O$ signal in the

(24) Borg, Ø.; Walmsley, J. C.; Dehghan, R.; Tanem, B. S.; Blekkan, E. A.; Eri, S.; Rytter, E.; Holmen, A. *Catal. Lett.* **2008**, *126*, 224–230.
(25) Borg, Ø.; Dietzel, P. D. C.; Spjelkavik, A. I.; Tveten, E. Z.; Walmsley, J. C.; Diplas, S.; Eri, S.; Holmen, A.; Rytter, E. *J. Catal.* **2008**, *259*, 161–164.
(26) Happel, J. *Chem. Eng. Sci.* **1978**, *33*, 1567–1568.
(27) Bennett, C. O. *Catal. Rev. Sci. Eng* **1976**, *13*, 121.
(28) Biloen, P. *J. Mol. Catal.* **1993**, *21*, 17–24.
(29) Shannon, S. L.; Goodwin, J. G. Jr. *Chem. Rev.* **1995**, *95*, 677–695.
(30) Vada, S.; Chen, B.; Goodwin, J. G. *J. Catal.* **1995**, *153*, 224–231.
(31) Van Dijk, H. A. J.; Hoebink, J. H. B. J.; Schouten, J. C. *Top. Catal.* **2003**, *26*, 111–119.
(32) Bertole, C. J.; Kiss, G.; Mims, C. A. *J. Catal.* **2004**, *223*, 309.
(33) Frøseth, V.; Holmen, A. *Top. Catal.* **2007**, *45*, 45–50.
(34) Lohitharn, N.; Goodwin, J. G. Jr. *J. Catal.* **2008**, *257*, 142–151.
(35) Govender, N. S.; Botes, F. G.; de Croon, M. H. J. M.; Schouten, J. C. *J. Catal.* **2008**, *260*, 254–261.
(36) Van der Lee, M. K.; Van Dillen, A. J.; Geus, J. W.; De Jong, K. P.; Bitter, J. H. *Carbon* **2006**, *44*, 629–637.
(37) Van der Lee, M. K.; Van Jos Dillen, A.; Bitter, J. H.; De Jong, K. P. *J. Am. Chem. Soc.* **2005**, *127*, 13573–13582.

***Table 1.*** Carbon Nanofiber Supported Cobalt Catalysts with Their Properties

| | cobalt precursor | impregnation solvent | Co loading (wt%) | particle size (nm)[a] | dispersion (%)[a] | Co surface atoms (mmol/gcat)[b] |
|---|---|---|---|---|---|---|
| 1 | $Co(NO_3)_2 \cdot 6H_2O$ | $H_2O$ | 22 | 16 | 6.0 | 0.22 |
| 2 | $Co(NO_3)_2 \cdot 6H_2O$ | $H_2O$ | 9.9 | 11 | 8.7 | 0.15 |
| 3 | $Co(NO_3)_2 \cdot 6H_2O$ | $H_2O$ | 13 | 8.5 | 11.3 | 0.25 |
| 4 | $Co(NO_3)_2 \cdot 6H_2O$ | EtOH | 7.5 | 5.9 | 16.3 | 0.22 |
| 5 | $Co(NO_3)_2 \cdot 6H_2O$ | EtOH | 5.4 | 5.3 | 18.1 | 0.17 |
| 6 | $Co(NO_3)_2 \cdot 6H_2O$ | EtOH | 3.7 | 4.7 | 20.4 | 0.13 |
| 7 | $Co(NO_3)_2 \cdot 6H_2O$ | EtOH | 1.1 | 4.5 | 21.3 | 0.04 |
| 8 | $Co(C_2H_3O_2)_2 \cdot 4H_2O$ | $H_2O$ | 4.2 | 4.1 | 23.4 | 0.18 |
| 9 | $Co(C_2H_3O_2)_2 \cdot 4H_2O$ | $H_2O$ | 0.9 | 2.9 | 33.1 | 0.05 |
| 10 | $Co(C_2H_3O_2)_2 \cdot 4H_2O$ | $H_2O$ | 1.0 | 2.6 | 36.9 | 0.06 |

[a] From quantitative XPS.[14] [b] Calculated from cobalt loading and dispersion.

backswitch was used to calculate the $OH_x$ coverage and residence time. The term $OH_x$ was introduced since this water transient originates from both O and OH intermediates as well as adsorbed $H_2O$ molecules. The H coverage was estimated from a switch from $^{12}CO/H_2/Kr$ to $^{12}CO/D_2/Ar$, which was also followed by a backswitch. In this case, however, the HD signal was used to estimate the hydrogen coverage.

To determine the presence of irreversibly bonded species, the initial transient (CO introduction) was measured for various Co particle sizes via two independent sets of experiments. In a first experiment, after cooling to 150 °C, CO was introduced via a switch from Ar (35 mL·min$^{-1}$) to $^{12}CO/Kr$ (1.5/33.5 mL·min$^{-1}$) at 1.85 bar. In a second experiment, after cooling to 210 °C, the CO introduction was performed by a switch from $H_2/Ar$ (15/35 mL·min$^{-1}$) to $^{12}CO/H_2/Kr$ (1.5/15/33.5 mL·min$^{-1}$). In both cases the transients of inert tracers, $^{12}CO$, and possible products were monitored with MS. Activities and selectivities obtained after these initial transients were identical to those of the SSITKA experiments described above.

## Results and Discussion

An overview of the catalysts used in this work and their properties is shown in Table 1.

In the steady-state isotopic transient kinetic analysis (SSITKA) experiments, methanation conditions ($H_2/CO = 10$) were applied. Since the cobalt particle size effect was found at Fischer−Tropsch conditions ($H_2/CO = 2$), first the relevance of the SSITKA experiments for FT conditions was investigated. Therefore, the surface-specific activity (TOF) of the cobalt catalysts during the SSITKA experiments was calculated based on the CO conversion and hydrocarbon formation. The TOF values, as a function of cobalt particle size, have been plotted in Figure 1.

From this graph, it can be concluded that the trend found with SSITKA (1.85 bar, $H_2/CO = 10$) agrees very well with the trend found earlier for FT conditions (1 and 35 bar, $H_2/CO = 2$). This indicates that the results obtained with SSITKA are relevant for FT conditions at 1 bar, as well as for industrial FT conditions at 35 bar.

The SSITKA experiments are also relevant for the methane selectivity found with FT conditions. Although the selectivity data were scattered and a high methane selectivity was found (78−84%) under SSITKA conditions, an indicative trend of an increase in $C_1$ selectivity with decreasing cobalt size (<6 nm) was observed. This is again in line with the trend in selectivity observed for the FT measurements conducted at 1 or 35 bar (see General Discussion section, Figure 8). Ethane and propane selectivities ranged 5.2−8.2 and 4.7−6.2 mol%, respectively.

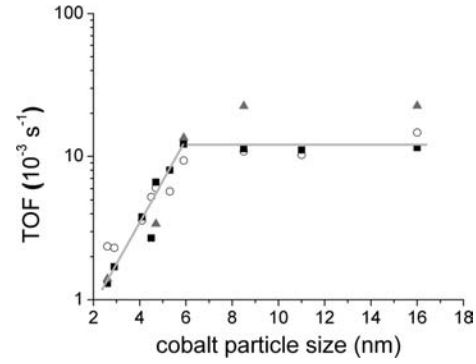


***Figure 1.*** Relation between cobalt particle size and TOF found at $H_2/CO = 2$: (■) 1 bar, 220 °C and (▲) 35 bar, 210 °C; and $H_2/CO = 10$: (○) 1.85 bar, 210 °C.

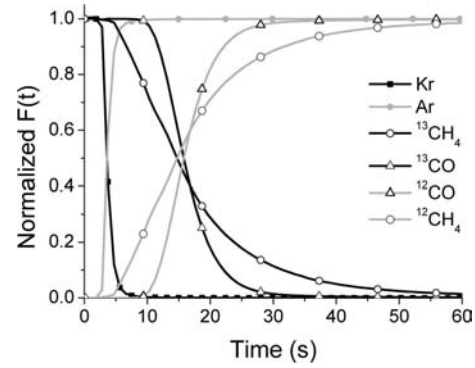


***Figure 2.*** Normalized transient curves from a $^{13}CO/H_2/Kr$ to $^{12}CO/H_2/Ar$ backswitch (catalyst 3, 8.5 nm).

**Reversibly Bonded $CH_x$ and CO Coverages and Residence Times.** Typical normalized transient curves obtained after a backswitch experiment (from $^{13}CO/H_2/Kr$ to $^{12}CO/H_2/Ar$) are depicted in Figure 2.

In this graph, it can be observed that the $CH_4$ transient signals change together with the change in the inert tracer transient signals. This indicates that, e.g., $^{12}CH_4$ is formed immediately after the isotopic backswitch ($^{13}CO/H_2/Kr$ to $^{12}CO/H_2/Ar$). In this paper, it suffices to treat the $CH_4$ transients as originating from a single carbon pool leading to $CH_4$. A more detailed analysis of these $CH_4$ transients can be found in the Supporting Information (SI)—SSITKA modeling - $CH_4$.

Regarding the CO transients, it can be observed that the decrease of the $^{13}CO$ signal and the concurring increase of $^{12}CO$ are steep but start later than the $CH_4$ signals. The latter observation can be ascribed to the fact that CO can readsorb on the cobalt surface (the so-called chromatographic effect),[39] in contrast to $CH_4$. A detailed analysis of the CO transients and the chromatographic effect is provided in the SI (SSITKA modeling - CO). To rule out the effect of the total cobalt surface area in the reactor, which might influence the number of adsorption/desorption possibilities and thus the CO residence times, a number of catalysts (2, 5, and 8 (Table 1)) were prepared with different loadings and particle sizes to have an approximately constant cobalt surface area per gram of catalyst. Therefore, both the amount of catalyst in the reactor and the bed residence time could be kept constant. The results found

(38) Frøseth, V.; Storsæter, S.; Borg, Ø.; Blekkan, E. A.; Rønning, M.; Holmen, A. *Appl. Catal., A* **2005**, *289*, 10–15.
(39) Biloen, P.; Helle, J. N.; van den Berg, F. G. A.; Sachtler, W. M. H. *J. Catal.* **1983**, *81*, 450–463.

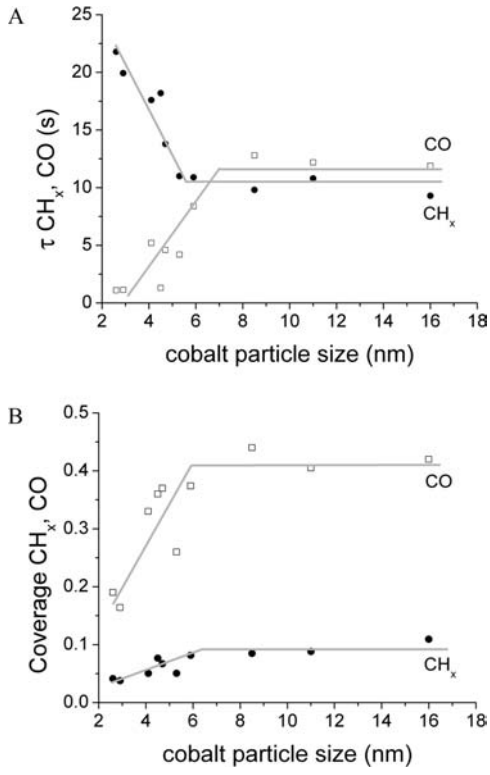


***Figure 3.*** (A) Corrected $CH_x$ (●) and CO (□) surface residence times as function of cobalt particle size (210 °C, 1.85 bar, $H_2/CO = 10$). (B) Coverage of reversibly bonded $CH_x$ and CO as function of cobalt particle size (210 °C, 1.85 bar, $H_2/CO = 10$).

for these catalysts did not deviate from the results found for the other catalysts listed in Table 1, which proved that the observed changes in residence times have to be ascribed to other effects.

From the analysis of the transient response curves, with eqs 1 and 2, the surface residence time $\tau$ (s) of $CH_x$ and CO were obtained as a function of the cobalt particle size.

As can be observed in Figure 3A, the surface residence time of $CH_x$ (representing carbon intermediates leading to methane) increased with decreasing cobalt particle size, for sizes smaller than 6 nm. The increase in $\tau_{CHx}$ might suggest that the smaller the cobalt particle size, the stronger the $CH_x$ species are bonded to the cobalt surface. Alternatively, it might point toward a hampered CO dissociation and/or a slower $CH_x$ hydrogenation. The CO residence time shows an opposite trend as compared to $\tau_{CH_x}$ and decreased for smaller particles (<6 nm). The CO and $CH_x$ residence times appeared to be independent of the particle size with sizes larger than 6 nm, with values in good agreement with those from literature.[38,40,41]

The surface coverages of reversibly bonded CO and $CH_x$ intermediates were calculated based on residence time, assuming a 1:1 ratio of CO and $CH_x$ to the Co surface atoms. As can be observed in Figure 3B, the surface coverages ($\theta$) of both CO and $CH_x$ decreased for Co particle sizes below 6 nm. In contrast, constant values were found for particle sizes larger than 6 nm. Based on these results it may seem that the total surface coverage of small (<6 nm) particles decreased. However, it should be stressed that the SSITKA experiments reveal exclusively the reversibly bonded intermediate species.

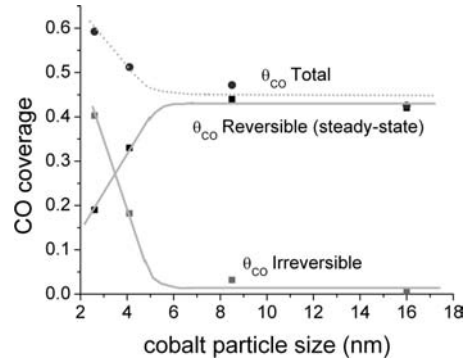


***Figure 4.*** CO coverage from CO introduction, reversibly (from steady-state measurements) and irreversibly bonded CO (210 °C, 1.85 bar, $H_2/CO = 10$).

**Total CO Coverage.** To check for the presence and the amount of irreversibly bonded species, the introduction of CO was monitored directly after *in situ* reduction. A difference between the amount of CO adsorbed during this CO introduction and the amount adsorbed found during SSTIKA is then to be ascribed to irreversibly bonded CO. The CO introduction transient was performed for a number of catalysts, at either 150 or 210 °C. A switch from Ar to $^{12}CO/Kr$ (at 150 °C) or from $H_2/Ar$ to $^{12}CO/H_2/Kr$ (at 210 °C) was made, while the MS signals from $^{12}CO$, Kr, Ar, $H_2O$, $^{12}CO_2$, and $^{12}CH_4$ were tracked. The CO coverage was calculated from these results as a function of the cobalt particle size.

In the first experiment performed at 150 °C, CO was introduced in the absence of $H_2$. From this experiment it was concluded that the CO coverage is constant ($\theta_{CO} = 0.51$) for Co particles larger than 6 nm (Figure SI.6). However, this value increases significantly for smaller particles, and a CO coverage of 0.93 is found for a Co particle size of 2.6 nm. This indicates that the $CO/Co_{surf}$ ratio is the highest for small particles. This might have been expected though, since a larger amount of edge/corner atoms for small particles compared to large ones provides a relative larger amount of linear CO adsorption possibilities. Another possible explanation would be the formation of subcarbonyls[42] on small cobalt particles.[43]

From the switch from $H_2/Ar$ to $CO/H_2/Kr$ at 210 °C, the total CO was calculated as a function of Co particle size (Figure 4) and compared with the coverage of the reversibly bonded CO from SSITKA. From the difference between those two coverages, the amount of irreversibly bonded CO was obtained.

This graph shows that the total CO coverage, deduced from the CO introduction experiment, increased with decreasing CO particle size (<6 nm). It has been shown already that the amount of reversibly bonded CO, found during steady-state isotopic switches, decreased for small cobalt particles. The difference between those two coverages reveals an increase in the irreversible $\theta_{CO}$ with decreasing particle size and hardly any irreversibly bonded CO for large particles (>6 nm). This means that under the present conditions the cobalt surface was partly blocked with unreactive CO for small particles, thereby hampering catalysis. This irreversible CO adsorption may be strong

(40) Schanke, D.; Vada, S.; Blekkan, E. A.; Hilmen, A. M.; Hoff, A.; Holmen, A. *J. Catal.* **1995**, *156*, 85–95.
(41) Kogelbauer, A.; Goodwin, J. G. Jr.; Oukaci, R. *J. Catal.* **1996**, *160*, 125–133.
(42) Moors, M.; de Bocarmé, T. V.; Kruse, N. *Catal. Today* **2007**, *124*, 61–70.
(43) Kuznetsov, V. L.; Aleksandrov, M. N.; Bulgakova, L. N. *J. Mol. Catal.* **1989**, *55*, 146–158.

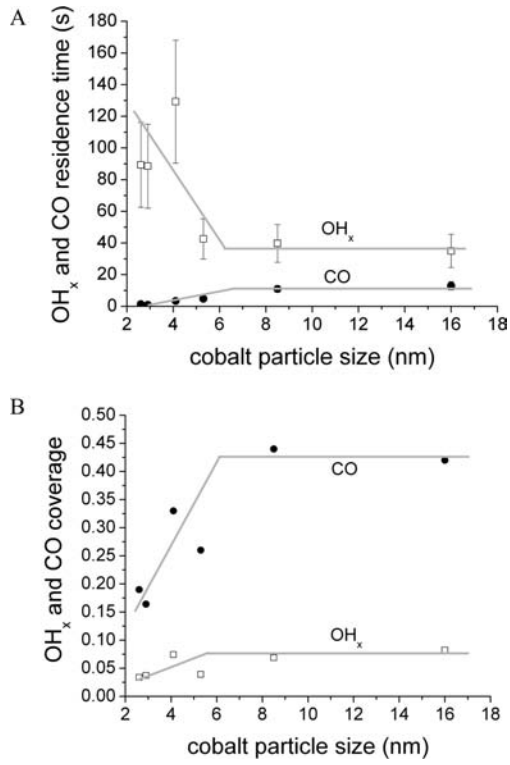


***Figure 5.*** (A) Residence times of reversibly bonded $^{18}OH_x$ and $C^{18}O$ as a function of cobalt particle size (210 °C, 1.85 bar, $H_2/CO = 10$). (B) Surface coverage of reversibly bonded $C^{18}O$ and $OH_x$ as a function of cobalt particle size (210 °C, 1.85 bar, $H_2/CO = 10$).

associative and/or dissociative chemisorption with strong Co−O and Co−C bonds.[44] The latter might even include strongly bonded $CH_x$ species. However, since hardly any $CO_2$ formation was detected for both large and small particles, we infer that the irreversibly bonded CO was mainly adsorbed molecularly.

**Residence Time and Coverage of Reversibly Bonded $OH_x$.** To determine the $OH_x$ residence time and coverage during the FT reaction, a switch from $C^{16}O/H_2/Ar$ to $C^{18}O/H_2/Kr$ was made, followed by a backswitch.

Although repeated isotopic switches showed substantially larger noise in the $H_2O$ transients compared to the $CH_4$ transients, a trend in $OH_x$ surface residence time can be discerned (Figure 5A). It appears that the $\tau_{OH_x}$ increased for Co particle sizes smaller than 6 nm. This suggests that smaller (<6 nm) cobalt particles bind $OH_x$ species stronger to the cobalt surface. It might also indicate a slower CO dissociation and/or $OH_x$ hydrogenation. A similar conclusion for a stronger Co−O bond could also be deduced from the $CO_2$ signals. (Figure SI.7) The $C^{18}O$ residence time and coverage showed the same trend and comparable values as $\tau_{^{13}CO}$ and $\theta_{^{13}CO}$.

The coverage of reversibly bonded $OH_x$ decreased for small particles, as observed for the $CH_x$ intermediates (Figure 5B). However, it has to be mentioned that the readsorption probability for water in the SSITKA apparatus is significantly larger than for methane and, thus, may yield too high values for residence time and surface coverage. Still, a trend of an increasing $\tau_{OH_x}$ and decreasing $\theta_{OH_x}$ value for small cobalt particles can be deduced.

**Hydrogen Coverages.** To estimate the H coverages, a switch from $^{12}CO/H_2/Kr$ to $^{12}CO/D_2/Ar$ (210 °C, 1.85 bar, $H_2/CO =$ 10) was made, followed by a backswitch after reaching isotopic steady state. Apart from the transients in $H_2$ and $D_2$, the signal from HD formed due to isotopic scrambling was monitored as well. A typical example of a $H_2-D_2$ switch experiment is depicted in Figure SI.8.

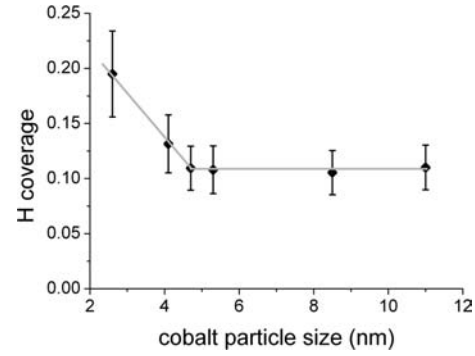


***Figure 6.*** Hydrogen coverage as function of the cobalt particle size (210 °C, 1.85 bar, $H_2/CO = 10$).

From this SSITKA experiment it was noticed that the transient in $H_2$ was faster than the inert tracer, which was observed for all the cobalt particle sizes. This is most likely caused by the faster diffusion rate of hydrogen compared to the inert gas, which made an estimation of the H residence time unattainable. Fortunately, the H coverage could be estimated from the formation of HD. The instantaneous HD formation showed a peak maximum at equal concentration of $H_2$ and $D_2$, while significant tailing was observed. Whereas the peak was attributed to adsorbed atomic hydrogen ($H_{ads}$), the tail could be a result of H-spillover and involvement of $CH_x$ and $OH_x$. Only the deconvoluted HD peak, without tail, was therefore used to estimate $\theta_H$ as function of the cobalt particle size (Figure 6). It should be noted that this yields the lower limit of the H coverage, since it assumes that all the $H_{ads}$ at the surface leaves it as HD. The amount of $H_2$ formed due to $H_{ads}$ recombination could not be detected, since no measurable difference between the $H_2$ transients from a blank experiment (reactor filled with CNF and SiC) and the above experiments was found.

From this graph it can be inferred that the H coverage increased for small Co particles. However, this means that the H/CO surface ratio was enhanced significantly from 0.2−0.3 (>5 nm) to 0.8 (2.6 nm) which may explain the increased methane selectivity for particles smaller than 6 nm.

## General Discussion

For the Fischer−Tropsch reaction several mechanisms have been put forward. Also, different rate determining steps, viz. CO dissociation and $CH_x$ hydrogenation, may apply. In this study it was assumed that the hydrogenation of $CH_x$ is rate limiting for all Co sizes. The TOF could then be calculated based on the SSITKA findings for residence time and coverage at $H_2/CO = 10$. The following kinetic expression can be used, assuming a pseudo-first-order reaction:

$$TOF_m = k_{CH_x}\theta_{CH_x} = \frac{1}{\tau_{CH_x}}\theta_{CH_x} \quad (4)$$

Using this formula, the $TOF_m$ was calculated for various cobalt particle sizes and compared with the TOF found at 1 and 35 bar. Please note that the SSITKA results were used as obtained and no fitting was involved.

From Figure 7, it can be observed that eq 4 gives a reasonable fit ($R^2 = 0.9$) to the observed TOF for FT

(44) Mavrikakis, M.; Bäumer, M.; Freund, H.-J.; Nørskov, J. K. *Catal. Lett.* **2002**, *81*, 153–156.

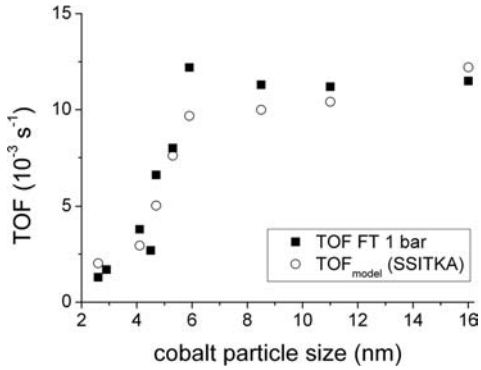


***Figure 7.*** Comparison of measured (FT, 1 bar, 220 °C, $H_2/CO = 2$) and modeled (SSITKA, 1.85 bar, 210 °C, $H_2/CO = 10$, eq 4) TOF.

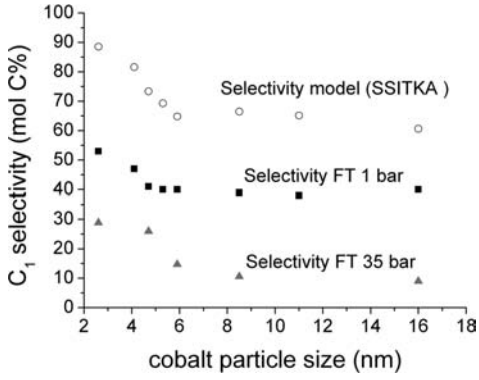


***Figure 8.*** Measured ($H_2/CO = 2$, 1 bar) and modeled methane selectivity based on SSITKA experiments ($H_2/CO = 10$, eq 7, $k_p/k_t = 0.3$).

conditions at 1 and 35 bar (compare Figure 1). This implies that the lower activity for small (<6 nm) particles is a result of a lower surface coverage and an increased residence time of the $CH_x$ intermediates.

The trend in methane selectivity could be described based on a termination (eq 5) and propagation (eq 6) reaction:

$$CH_3 + H \rightarrow CH_4 \quad (5)$$

$$CH_3 + CH_2 \rightarrow C_2H_5 \quad (6)$$

Using these reactions, the following equation for the selectivity is proposed, assuming that both $CH_3$ as $CH_2$ can be described as $CH_x$.

$$S = \frac{r_t}{r_t + r_p} = \frac{k_t \theta_{CH_x} \theta_H}{k_t \theta_{CH_x} \theta_H + k_p \theta_{CH_x} \theta_{CH_x}} = \frac{\theta_H}{\theta_H + \frac{k_p}{k_t} \theta_{CH_x}} \quad (7)$$

The ratio of the propagation and termination constant ($k_p/k_t$) was estimated by fitting the data to the measured selectivity (Figure 8), assuming the $k_p/k_t$ ratio to be constant for all particle sizes.

From this graph, it appears that the trend in $C_1$ selectivity can be obtained from the coverages found with SSITKA. The fact that the absolute values in methane selectivity from the SSITKA model and the FT experiments are different is due to the higher $H_2/CO$ ratio of the SSITKA conditions.

Clearly, the FT activity and selectivity can be modeled quantitatively and qualitatively, respectively, based on the SSITKA experiments. This means that it is possible with this technique to deconvolute the TOF into its separate contributions regarding coverages and residence times.

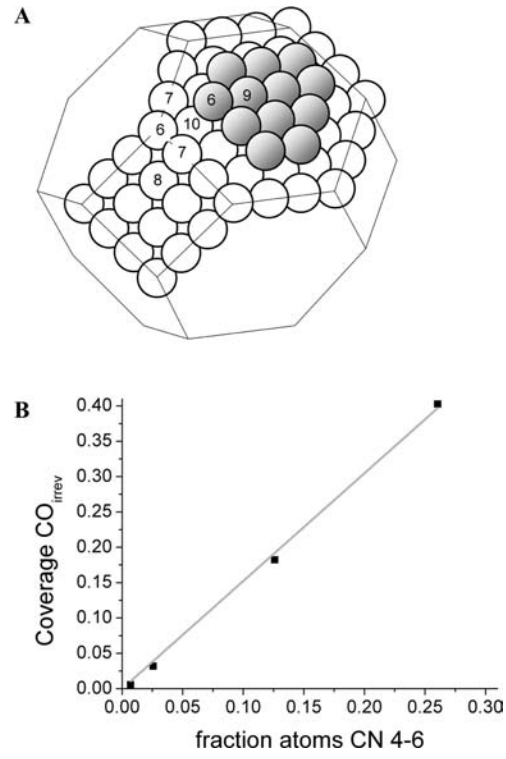


***Figure 9.*** (A) Geometric model with some coordination numbers (reproduced from ref 45). (B) Coverage of irreversibly bonded CO as function of the fractions of atoms with coordination number 4−6 (using results from catalysts 1, 3, 8, and 10).

Next, we attempted to provide a possible explanation for the observed changes of residence times and coverages with the cobalt surface structure as a function of particle size. To this end, the cobalt particles were described with a geometric, cuboctahedral model[45,46] (Figure 9A). Based on this model, the fraction of surface atoms with a specific coordination number (CN) could be calculated as a function of the cobalt particle size. The cobalt surface atoms with CN values of 4−6 and 7−11 were summed up and referred to as corner and terrace atoms, respectively. After that, the fraction of atoms exhibiting a coordination number ranging from 4 to 6 was plotted versus the fraction of irreversibly chemisorbed CO (Figure 9B).

As shown in Figure 9B, a linear relation between the fraction of cobalt surface atoms with a low coordination number (CN = 4−6) and the coverage of irreversibly bonded CO is obtained. Based on this result we speculate that the increase in irreversibly bonded CO for small (<6 nm) Co particles is related to the increase in coordinatively unsaturated site (cus) atoms.[47]

The fact that the slope of the curve is larger than unity might be explained by a CO/Co > 1 adsorption ratio for corner and edge atoms. Also, the invasive character of CO may roughen the cobalt surface,[48] which is ignored in this static geometric model.

The reason for the stronger or irreversible CO bonding by the surface atoms with a low coordination number may be due to an increased localization of the valence electrons. This localization brings about the center of the d-band to shift upward

(45) Van Hardeveld, R.; Hartog, F. *Surf. Sci.* **1969**, *15*, 189–230.
(46) Poltorak, O. M.; Boronin, V. S. *Russ. J. Phys. Chem.* **1966**, *40*, 1436–1445.
(47) Schlögl, R.; Abd Hamid, S. B. *Angew. Chem., Int. Ed.* **2004**, *43*, 1628–1637.
(48) Wilson, J.; De Groot, C. *J. Phys. Chem.* **1995**, *99*, 7860–7866.

and, thereby, a stronger binding of adsorbates as CO and dissociated C and O atoms to the surface.[44,49,50] Apart from this local electronic effect, also the decrease in Fermi level with decreasing metal crystallite size (<7 nm) can be used to explain the stronger CO adsorption for smaller cobalt particles.[22,51] This effect was also found in a theoretical study by Reboredo and Galli which showed that the CO adsorption energy increased significantly with decreasing Co cluster size.[52]

Despite the higher CO adsorption energy at small Co particles, the more convex surface of those particles will make CO dissociation more difficult. Moreover, since hardly any $CO_2$ formation was detected during the CO introduction experiment we think that the irreversibly bonded CO is associatively chemisorbed and does not take part in the FT reaction.

The highest coverage of $CO_{irrev}$ found for the smallest Co particle size amounts to roughly 50% of the total surface coverage. Since the TOF is based on total surface Co atoms, this would lead to a factor of 2 drop if the free sites would keep their specific activity. However, the observed decrease in TOF equals a factor of ~10 (Figure 7), which means that a significant effect originates from a lower specific activity of terrace sites. Please note that the coverages of reversibly bonded $CH_x$ and CO drop by ~50% for the smallest Co particles (Figure 3B). The coverages of these species based on terrace sites only, therefore, remain constant for all Co particle sizes. This lower activity of terrace sites is thus caused by a slower $CH_x$ hydrogenation step and/or hampered CO dissociation as revealed by the higher $CH_x$ residence times for smaller particles. Since metal particles larger than 2 nm are expected to show a metallic character, the question is why those reactions would occur slower on a terrace at a small Co particle compared to a terrace at a large one. Part of the answer might overlap with the explanation used above for the irreversible CO adsorption. The presence of a significant amount of cus atoms on small Co particles might influence the electronic properties of neighboring terrace atoms, thereby decreasing their activity. It is also feasible that either the strongly bonded CO and $CH_x$ intermediates or the particle geometry limits the formation of CO reservoirs[53] and hampers surface reconstruction.[54] This surface reconstruction could lead to surface steps and kinks[55,56] or so-called B5 sites[4,45,57,58] which are known for their ability to facilitate CO dissociation, $CH_x$ hydrogenation,[59] and C−C bond formation.[60] The slower $CH_x$ hydrogenation could be caused by a too strong Co−$CH_x$ bond. This is in line with a thermodynamical model which rationalized an increase in the heat of adsorption of reactants and intermediates with decreasing particle size.[61,62]

## Conclusions

A cobalt particle size effect has been shown in the Fischer−Tropsch catalysis previously. For Co particles smaller than 6 nm, a decreased TOF and increased methane selectivity has been found for FT experiments performed at 1 and 35 bar ($H_2/CO = 2$). The same trend was observed in the current SSITKA experiments (1.85 bar, $H_2/CO = 10$), implying that this technique could be used to investigate the cobalt particle size effects.

From the SSITKA experiments it was concluded that the surface residence times of reversibly bonded $CH_x$ and $OH_x$ intermediates increased significantly for particles smaller than 6 nm, whereas a decrease was observed for the CO residence time. The $CH_x$, $OH_x$, and CO residence times appeared independent of size for larger Co particles (>6 nm).

The surface coverages of the $CH_x$, $OH_x$ and CO intermediates decreased for small particles and appeared to be constant for large particles. On the contrary, an increase in H coverage was observed for small (<6 nm) Co particles. From CO introduction experiments it was concluded that a significant amount of irreversibly bonded CO molecules is present on small particles too, causing blocking of part of the Co surface.

The SSITKA results on coverages and residence times were used to model the trend in TOF and methane selectivity as obtained under FT conditions. It was concluded that the lower TOF found for small cobalt particles (<6 nm) compared to larger ones is the result of a significant increase in the $CH_x$ residence time combined with a decrease of the $CH_x$ coverage. The higher methane selectivity of small Co particles obtained with FT conditions was mainly rationalized from the higher coverage of hydrogen.

The current SSITKA study can be regarded as a major step forward in understanding the origin of cobalt particle size effects in the Fischer−Tropsch catalysis. The methodology used provides fundamental insight in the performance−size relation and, therefore, might be applied for studies of particle size effects in general.

**Acknowledgment.** The authors kindly acknowledge Shell Global Solutions for financial support.

**Supporting Information Available:** Full details on modeling of $CH_4$ and CO transient curves, CO coverage during its introduction at 150 °C, and examples of CO, $CO_2$, and HD transients as a function of cobalt particle size. This material is available free of charge via the Internet at http://pubs.acs.org.

JA901006X

(49) Mavrikakis, M.; Hammer, B.; Nørskov, J. K. *Phys. Rev. Lett.* **1998**, *81*, 2819.
(50) Henry, C. R.; Chapon, C.; Goyhenex, C.; Monot, R. *Surf. Sci.* **1992**, *272*, 283–288.
(51) Wood, D. M. *Phys. Rev. Lett.* **1981**, *46*, 749.
(52) Reboredo, F. A.; Galli, G. *J. Phys. Chem. B* **2006**, *110*, 7979–7984.
(53) Oosterbeek, H. *Phys. Chem. Chem. Phys.* **2007**, *9*, 3570–3576.
(54) Ciobîca, I. M.; van Santen, R. A.; van Berge, P. J.; van de Loosdrecht, J. *Surf. Sci.* **2008**, *602*, 17–27.
(55) Ge, Q.; Neurock, M. *J. Phys. Chem. B* **2006**, *110*, 15368–15380.
(56) Huo, C.-F.; Li, Y.-W.; Wang, J.; Jiao, H. *J. Phys. Chem. C* **2008**, *112*, 14108–14116.
(57) Wortman, R.; Gomer, R.; Lundy, R. *J. Chem. Phys.* **1957**, *27*, 1099.
(58) Chorkendorff, I.; Niemantsverdriet, J. W. In *Concepts of Modern Catalysis and Kinetics*; Wienheim/Wiley-VCH: New York, 2003; pp 301−348.
(59) Cheng, J.; Gong, X.-Q.; Hu, P.; Lok, C. M.; Ellis, P.; French, S. *J. Catal.* **2008**, *254*, 285–295.
(60) Cheng, J.; Hu, P.; Ellis, P.; French, S.; Kellys, G.; Lok, C. M. *J. Phys. Chem. C* **2008**, *112*, 6082–6086.
(61) Parmon, V. N. *Dokl. Phys. Chem.* **2007**, *413*, 42–48.
(62) Murzin, D. Y. *Chem. Eng. Sci.* **2009**, *64*, 1046–1052.